ROZPRAWY INŻYNIERSKIE • ENGINEERING TRANSACTIONS • 31, 3, 293—315, 1983
Polska Akademia Nauk • Instytut Podstawowych Problemów Techniki

MIXED BOUNDARY VALUE PROBLEMS OF A TRANSVERSELY ISOTROPIC LAYER UNDER TORSION AND VARIOUS BOUNDARY CONDITIONS

B. ROGOWSKI (ŁÓDŹ)

This paper deals with the axially symmetric torsion of a transversely isotropic layer elastically supported at the lower plane or bonded with dissimilar half-space. Two types of the three-part mixed boundary value problems are considered: flat annular crack problem and annular torsional indentation problem. Numerical results are discussed and displayed graphically.

1. INTRODUCTION

The classical Reissner-Sagoci problem [1–3] and penny-shaped crack problem [4] have been extended by several investigators to accomodate a variety of effects, especially on the indentation of a solid by a rigid annulus [5–10], the annular crack problems [11–14] involving infinite or semi-infinite bodies of particular anisotropic elastic materials [15–19]. Therefore the closed-form solutions have been obtained in the classical problems [2, 4].

The crack and contact problems involving annular region are reduced to a solution of the Fredholm integral equation of the first kind. An attempt is made to solve the equation by an iterative procedure [6, 9, 20] or by an approximate method [13, 21]. The three-part mixed boundary value problem, on the other hand, is reduced to the solution of an infinite system of simultaneous equations [10–12]. For isotropic bodies of finite extent, these problems have been attacked for a thick plate [22–24] and for a layer bonded to a half-space [25].

Conventional stress analysis for anisotropic materials is considerably more complex than in the corresponding isotropic theory, but some annular contact and crack problems involving infinite or semi-infinite bodies of particular anisotropic materials have been successively examined [15–19].

In the present paper the author solves title problems in the framework of the theory of anisotropic elasticity by means of Hankel's transforms and triple integral equations. In Sect. 2 the stress and displacement states are obtained for the cases as the lower surface of the layer is stress free or rigid clamped or elastically clamped or perfectly bonded to a dissimilar transversely isotropic half-space and the upper surface of the layer is loaded under torsion or when the tangential, circumferential displacement is fixed. The torsion of an internal annular crack located in the middle

plane of the layer or bi-material composite is considered in Sect. 3. The solution preserves the essential feature of singular stress field mear the crack tips and the stress intensity factors are easily evaluated. The torsional indentation of a layer elastically or rigid clamped at a lower plane and of a bi-material composite by an embedded rigid annulus is considered in Sect. 4.

Triple integral equations of the problems are solved by expansion of the displacement (in the crack problem) and of the contact streses (in the contact problem) into a Fourier series (with singularities of the interaction at the edges of the contact region), which leads to a system of an infinite number of simultaneous algebraic equations, i.e. extending the method of SHIBUYA *et al.* [10, 11]. These equations are solved by truncation and several numerical results for some practicals materials such as magnesium and cadmium single crystals and fiber-reinforced composites are given and compared with those of the isotropic material to show the effect of anisotropy, boundary conditions and the geometric configuration of the problems.

2. BASIC EQUATIONS AND THEIR SOLUTION

A cylindrical coordinate system (r, θ, z) is used with the z-axis coinciding with the axis of geometric and material symmetry of the transversely isotropic body. Since the problem considered here is one of axially symmetric torsion, the only nonvanishing component of displacement is v_θ and the stresses are $\sigma_{\theta z}$ and $\sigma_{r\theta}$. These stresses and displacement can be expressed in the elastostatic problem in terms of the displacement potential from the relations [26]

$$(2.1)\qquad v_\theta = -\frac{\partial \varphi}{\partial r}, \quad \sigma_{\theta z} = -G_z \frac{\partial^2 \varphi}{\partial r\, \partial z}, \quad \sigma_{r\theta} = G_z \frac{\partial^2 \varphi}{\partial z^2} + 2G \frac{1}{r} \frac{\partial \varphi}{\partial r},$$

in which G and G_z denote the shear modulus in the $r-\theta$ plane (isotropic) and in the z-axis direction, respectively, $\varphi(r, z)$ is the displacement potential and is a solution of the partial differential equation

$$(2.2)\qquad \left(\frac{\partial^2}{\partial r^2} + \frac{1}{r}\frac{\partial}{\partial r} + \frac{1}{s^2}\frac{\partial^2}{\partial z^2}\right)\varphi(r, z) = 0, \quad s^2 = \frac{G}{G_z}.$$

Suitable solutions of Eq. (2.2) are taken in the form

$$(2.3)\qquad \varphi(r, z) = \int_0^\infty [A(\xi) \operatorname{ch} s\xi (z-h) + B(\xi) \operatorname{sh} s\xi (z-h)] J_0(\xi r)\, d\xi,$$

$$(2.4)\qquad \varphi'(r, z) = \int_0^\infty C(\xi) \exp[-s'\xi (z-h)] J_0(\xi r)\, d\xi, \quad s' = \left(\frac{G'}{G_z'}\right)^{\frac{1}{2}},$$

for the layer $0 \leqslant z \leqslant h$ and for the half-space $z \geqslant h$, respectively, where $J_n(\xi r)$ is the Bessel function of the first kind of order n and $A(\xi)$, $B(\xi)$, $C(\xi)$ are arbitrary functions of ξ.

The displacement and shear stresses corresponding to the potentials (2.3) or (2.4) are given by

$$\sigma_{z\theta}=G_{\text{arg}}\int_0^\infty \xi^2\,[A(\xi)\,\text{sh}\,s\xi\,(z-h)+B(\xi)\,\text{ch}\,s\xi\,(z-h)]\,J_1(\xi r)\,d\xi,$$

$$\sigma_{r\theta}=-G\int_0^\infty \xi^2\,[A(\xi)\,\text{ch}\,s\xi\,(z-h)+B(\xi)\,\text{sh}\,s\xi\,(z-h)]\,J_2(\xi r)\,d\xi, \tag{2.5}$$

$$v_\theta=\int_0^\infty \xi\,[A(\xi)\,\text{ch}\,s\xi\,(z-h)+B(\xi)\,sh\,s\xi\,(z-h)]\,J_1(\xi r)\,d\xi,$$

for the layer with the material parameters G, G_z and

$$\sigma'_{z\theta}=-G'_{\text{arg}}\int_0^\infty \xi^2\,C(\xi)\exp[-s'\xi\,(z-h)]\,J_1(\xi r)\,d\xi,$$

$$\sigma'_{r\theta}=-G'\int_0^\infty \xi^2\,C(\xi)\exp[-s'\xi\,(z-h)]\,J_2(\xi r)\,d\xi, \tag{2.6}$$

$$v'_\theta=\int_0^\infty \xi\,C(\xi)\exp[-s'\xi\,(z-h)]\,J_1(\xi r)\,d\xi,$$

for the half-space with the material parameters G', G'_z, in which G_{arg} and G'_{arg} denote the average shear modulus

$$G_{\text{arg}}=\sqrt{G\,G_z}\,. \tag{2.7}$$

We assume that the surface $z=h$ of the layer $0\leqslant z\leqslant h$ is elastically supported or the other case, when the layer is bonded with a surrounding material (transversely isotropic half-space) when the interface at $z=h$ is idealized such that the stress and displacement are continuous. Then we consider the following two boundary conditions:

$$\sigma_{z\theta}(r,h)=-kv_\theta(r,h). \tag{2.8}$$

$$\sigma_{z\theta}(r,h)=\sigma'_{z\theta}(r,h),\qquad v_\theta(r,h)=v'_\theta(r,h). \tag{2.9}$$

The unknowns in Eqs. (2.5) and (2.6) are not independent in view of Eqs. (2.8) or (2.9) which, when enforced, yield

$$B(\xi)=-\kappa_1(\xi h)^{-1}A(\xi), \tag{2.10}$$

where

$$\kappa_1=kh\,G_{\text{arg}}^{-1}, \tag{2.11}$$

or

$$B(\xi)=-\kappa_0\,C(\xi),\qquad A(\xi)=C(\xi), \tag{2.12}$$

where

$$\kappa_0=G'_{\text{arg}}\,G_{\text{arg}}^{-1}. \tag{2.13}$$

Substituting Eqs. (2.10) or (2.12) into Eqs. (2.5), we get

$$\sigma_{z\theta}=G_{\mathrm{arg}}\int_0^\infty \xi^2 A(\xi)\,[\mathrm{sh}\, s\xi(z-h)-\kappa_i(\xi h)^{-i}\,\mathrm{ch}\, s\xi(z-h)]\,J_1(\xi r)\,d\xi,$$

$$\sigma_{r\theta}=-G\int_0^\infty \xi^2 A(\xi)\,[\mathrm{ch}\, s\xi(z-h)-\kappa_i(\xi h)^{-i}\,\mathrm{sh}\, s\xi(z-h)]\,J_2(\xi r)\,d\xi, \tag{2.14}$$

$$v_\theta=\int_0^\infty \xi A(\xi)\,[\mathrm{ch}\, s\xi(z-h)-\kappa_i(\xi h)^{-i}\,\mathrm{sh}\, s\xi(z-h)]\,J_1(\xi r)\,d\xi, \qquad i=0,1,$$

where $i=1$ corresponds to the condition (2.8) and $i=0$ to the condition (2.9). In the second case of boundary conditions the displacement and stress states in the half-space are given by the formulas (2.6) for $C(\xi)=A(\xi)$.

It should be noted that the boundary condition (2.8) presents general boundary conditions of the system. When $k=0$, the layer is free at the lower edge, when $k=\infty$, the layer is clamped at one and when the spring of stiffness k is nonzero and bounded, the layer is elastically clamped at $z=h$.

Now we define the functions $v(\xi)$ or $t(\xi)$ such that

$$v(\xi)=A(\xi)\,[\mathrm{ch}\, s\xi h+\kappa_i(\xi h)^{-i}\,\mathrm{sh}\, s\xi h], \qquad i=0,1 \tag{2.15}$$

or

$$t(\xi)=-\xi A(\xi)\,[\mathrm{sh}\, s\xi h+\kappa_i(\xi h)^{-i}\,\mathrm{ch}\, s\xi h], \qquad i=0,1. \tag{2.16}$$

Then the stress and displacement components from Eqs. (2.14) are

$$\sigma_{z\theta}=-G_{\mathrm{arg}}\int_0^\infty \xi^2 v(\xi)\,\{[1-M_i(\xi h)]\,\mathrm{ch}\, s\xi z-\mathrm{sh}\, s\xi z\}\,J_1(\xi r)\,d\xi,$$

$$\sigma_{r\theta}=-G\int_0^\infty \xi^2 v(\xi)\,\{\mathrm{ch}\, s\xi z-[1-M_i(\xi h)]\,\mathrm{sh}\, s\xi z\}\,J_2(\xi r)\,d\xi, \tag{2.17}$$

$$v_\theta=\int_0^\infty \xi v(\xi)\,\{\mathrm{ch}\, s\xi z-[1-M_i(\xi h)]\,\mathrm{sh}\, s\xi z\}\,J_1(\xi r)\,d\xi, \qquad 0\leqslant z\leqslant h,$$

or

$$\sigma_{z\theta}=G_{\mathrm{arg}}\int_0^\infty \xi t(\xi)\,\{\mathrm{ch}\, s\xi z-[1-H_i(\xi h)]\,\mathrm{sh}\, s\xi z\}\,J_1(\xi r)\,d\xi,$$

$$\sigma_{r\theta}=G\int_0^\infty \xi t(\xi)\,\{[1-H_i(\xi h)]\,\mathrm{ch}\, s\xi z-\mathrm{sh}\, s\xi z\}\,J_2(\xi r)\,d\xi, \tag{2.18}$$

$$v_\theta=-\int_0^\infty t(\xi)\,\{[1-H_i(\xi h)]\,\mathrm{ch}\, s\xi z-\mathrm{sh}\, s\xi z\}\,J_1(\xi r)\,d\xi, \qquad 0\leqslant z\leqslant h,$$

where the functions $M_i(x)$ and $H_i(x)$ ($x=\xi h$) are defined by the following equations:

$$M_i(x)=\begin{cases}2(x-\kappa_1)\,[e^{2sx}(x+\kappa_1)+x-\kappa_1]^{-1}, & i=1,\\ 2(1-\kappa_0)\,[e^{2sx}(1+\kappa_0)+1-\kappa_0]^{-1}, & i=0,\end{cases} \tag{2.19}$$

$$H_i(x)=\begin{cases}-2(x-\kappa_1)\,[e^{2sx}(x+\kappa_1)-(x-\kappa_1)]^{-1}, & i=1,\\ -2(1-\kappa_0)\,[e^{2sx}(1+\kappa_0)-(1-\kappa_0)]^{-1}, & i=0,\end{cases} \tag{2.20}$$

respectively, to the elastically clamped edge $z=h$ ($i=1$) and for the case when the surface $z=h$ of the layer is bonded with the half-space $z\geqslant h$ ($i=0$).

The functions $M_i(x)$ and $H_i(x)$ are dependent on the parameters κ_1 or κ_0 (given by Eqs. (2.11) and (2.13)) and the material parameter $s\in R_+$. These functions, for arbitrary values of the elastic constants, have the properties

$$\lim_{x\to 0} e^{2sx}\{M_i(x), H_i(x)\}=\begin{cases}\left\{2\left(1-\dfrac{2\kappa_0}{1+\kappa_0}\,\delta_{i0}\right), \quad -2\left(1-\dfrac{2\kappa_0}{1+\kappa_0}\,\delta_{i0}\right)\right\} & \\ \qquad\qquad\qquad\qquad\qquad\qquad (\kappa_i \text{ bounded}),\\ \{-2,2\} \quad (\kappa_i\to\infty), \quad \delta_{i0}=\begin{cases}1, & i=0,\\ 0, & i=1,\end{cases}\end{cases}$$

$$M_0(0)=1-\kappa_0\ (\kappa_0 \text{ bounded}), \quad \lim_{x\to\infty} M_0(x)=-s^{-1} \quad (\kappa_0\to\infty),$$

$$\lim_{x\to 0} xM_1(x)=-\frac{\kappa_1}{1+s\kappa_1}, \quad H_i(0)=1-\kappa_i^{i-1} \quad (\kappa_0\neq 0), \tag{2.21}$$

$$M_0(x,\kappa_0=1)=H_0(x,\kappa_0=1)=0;$$

$\bigwedge_{\kappa_i,\,x\in R_+}$ $M_i(x)$ and $H_i(x)$ are the continuous functions.

For the properties (2.21) of the functions $M_i(x)$ and $H_i(x)$ the solution of the problems are bounded for any parameter κ_0, κ_1, s (in the boundary conditions on the upper plane of the layer there may be cases that κ_1 must be nonzero, e.g. the torsional indentation problem) and the infinite integrals (2.17) and (2.18) are convergent; we can easily evaluate these integrals by a numerical method. The functions $M_i(x)$ and $H_i(x)$ are identically zero when h tends to infinity. The functions $M_0(x)$ and $H_0(x)$ are also identically zero when the parameter $\kappa_0=1$, i.e. as

$$GG_z=G'G_z' \tag{2.22}$$

and the stress and displacement distributions in the layer and in the half-space, in this case, are the same as for a semi-infinite medium with the corresponding elastic constants G, G_z and G', G_z'. The physical quantities on the surface $z=0$ ($\sigma_{z\theta}$, v_θ), in this case, have the same values as in the case of a homogeneous solid.

The displacement and stress components at $z=0$ are

$$\sigma_{z\theta}(r,0)=-G_{\text{arg}}\int_0^\infty \xi^2 v(\xi)\,[1-M_i(\xi h)]\,J_1(\xi r)\,d\xi,$$

$$\sigma_{r\theta}(r,0)=-G\int_0^\infty \xi^2 v(\xi)\,J_2(\xi r)\,d\xi, \tag{2.23}$$

$$v_\theta(r,0)=\int_0^\infty \xi v(\xi)\,J_1(\xi r)\,d\xi$$

or

$$\sigma_{z\theta}(r,0)=G_{\text{arg}}\int_0^\infty \xi t(\xi)\,J_1(\xi r)\,d\xi,$$

$$\sigma_{r\theta}(r,0)=G\int_0^\infty \xi t(\xi)\,[1-H_i(\xi h)]\,J_2(\xi r)\,d\xi, \tag{2.24}$$

$$v_0(r,0)=-\int_0^\infty t(\xi)\,[1-H_i(\xi h)]\,J_1(\xi r)\,d\xi.$$

The solutions of two types of mixed boundary value problems will be presented in the next sections on the basis of the results of this section. In the first problem the displacement and stress distributions in the vicinity of the annular crack and the fracture parameters are analysed while in the second the torsional indentation problem of a transversely isotropic layer or bi-material composite system by an embedded rigid annulus is considered. The mathematical technique follows the one developed in [10, 11].

3. Layer containing an annular crack under torsion

We consider the elastic transversely isotropic layer $\Omega=\{(r,\theta,z)\colon 0\leqslant r<\infty,\ 0\leqslant\theta\leqslant 2\pi,\ |z|\leqslant h\}$ containing a flat annular crack $S=\{(r,\theta,0)\colon a\leqslant r\leqslant b,\ 0\leqslant\theta\leqslant 2\pi\}$, located in the middle plane of the layer. The crack surface is subjected to an axisymmetric distribution of tangential traction $\tau_0 r$, where τ_0 is constant. At the edges of the layer $|z|=h$ we will consider two types of boundary conditions: elastically clamped edges or as its edges are perfectly bonded to half-spaces Ω^+ $(z\geqslant h)$ and Ω^- $(z\leqslant -h)$. In the second problem the materials of the layer and the half-spaces are different but homogeneous, transversely isotropic and elastic. For the sake of convenience only, we shall assume that the unit of length is such that the outer radius of the crack is 1 and the inner radius is $\lambda=a/b$. Using the dimensionless variables and parameters defined by $\rho=r/b$, $\zeta=z/b$, $\eta=h/b$, $\xi h=x\eta$, the fundamental equations and boundary conditions are expressed below in these dimensionless coordinates. Since the problem is symmetrical with respect to the plane $z=0$, it is sufficient to consider only the solution for the layer $0\leqslant z\leqslant h$ with the boundary

conditions (2.8) or (2.9), considered above, in the plane $z=h$ and with conditions specified on $z=0$ inside and outside the segment $\lambda<\rho<1$

$$\sigma_{z\theta}(\rho, 0)=-b\rho\tau_0, \quad \lambda<\rho<1, \tag{3.1}$$

$$v_0(\rho, 0)=0, \quad 0\leqslant\rho\leqslant\lambda, \quad 1\leqslant\rho. \tag{3.2}$$

Using Eqs. (2.23), it can be shown that the function $v(x)$ is the only unknown from Eqs. (3.1) and (3.2) which can be found from the triple integral equations

$$\int_0^\infty x^2 v(x)[1-M(x\eta)]J_1(x\rho)\,dx=\rho\frac{\tau_0 b}{G_{arg}}, \quad \lambda<\rho<1, \tag{3.3}$$

$$\int_0^\infty xv(x)J_1(x\rho)\,dx=0, \quad 0\leqslant\rho\leqslant\lambda, \quad 1\leqslant\rho. \tag{3.4}$$

The functions $M(x\eta)$ are given by Eqs. (2.19); for elastically clamped edges it is $M(x)=M_1(x)$ and for the bi-material composite it is $M(x)=M_0(x)$. Being able to determine the unknown function $v(x)$ in the triple integral equations (3.3) and (3.4), we will get a solution satisfying all the boundary conditions. However, in general, it is very difficult to obtain a closed-form solution for the above equations. We use the analytical method; these equations are solved by expansion of the displacement v_θ of the crack surface into a Fourier series, which leads to a system of an infinite number of simultaneous algebraic equations.

The interval $\lambda\leqslant\rho\leqslant1$ corresponds to $0\leqslant\alpha\leqslant\pi$, as

$$\alpha=\arccos\left(1-2\frac{\rho^2-\lambda^2}{1-\lambda^2}\right), \tag{3.5}$$

when $\rho=\lambda$ corresponds to $\alpha=0$ and $\rho=1$ to $\alpha=\pi$.

Denoting

$$Z_n(x)=J_n\left(x\frac{1+\lambda}{2}\right)J_n\left(x\frac{1-\lambda}{2}\right) \tag{3.6}$$

and using the integral formula [27]

$$\int_0^\infty xJ_0(x\rho)Z_n(x)\,dx=\begin{cases}0, & 0\leqslant\rho<\lambda, \quad 1<\rho,\\ \dfrac{4}{\pi(1-\lambda^2)}\cdot\dfrac{\cos n\alpha}{\sin\alpha}, & \lambda<\rho<1,\end{cases} \tag{3.7}$$

we get

$$\int_0^\infty xJ_1(x\rho)\frac{\partial Z_n(x)}{\partial x}\,dx=-\rho\int_0^\infty xJ_0(x\rho)Z_n(x)\,dx=\begin{cases}0, & 0\leqslant\rho<\lambda, \quad 1<\rho,\\ \dfrac{-4\rho}{\pi(1-\lambda^2)}\cdot\dfrac{\cos n\alpha}{\sin\alpha}, & \lambda<\rho<1,\end{cases} \tag{3.8}$$

$$\int_0^\infty J_1(x\rho)Z_n(x)\,dx=\begin{cases}0, & 0\leqslant\rho\leqslant\lambda, \quad 1\leqslant\rho,\\ \dfrac{\sin(n\alpha)}{\pi n\rho}, & \lambda\leqslant\rho\leqslant1, \quad n=1, 2, 3, \ldots.\end{cases} \tag{3.9}$$

Then the unknown function $v(x)$ and the displacement $v_\theta(\rho)$ on the crack surface can be expressed by series:

$$xv(x)=\frac{\tau_0 b(1-\lambda^2)}{8G_{arg}}\sum_{n=1}^{\infty} a_n Z_n(x), \tag{3.10}$$

$$v_\theta(\rho,0)=\frac{\tau_0 b^2(1-\lambda^2)}{8\pi G_{arg}}\begin{cases}0 & , \quad 0\leqslant\rho\leqslant\lambda, \quad 1\leqslant\rho,\\ \dfrac{1}{\rho}\displaystyle\sum_{n=1}^{\infty}\frac{a_n}{n}\sin(n\alpha), & \lambda<\rho<1.\end{cases} \tag{3.11}$$

Thus the boundary condition on $v_\theta(\rho)$ is satisfied for any value of a_n and the displacement on the crack surface is expressed by the Fourier sine series (3.11). Therefore, to determine the coefficients a_n, we use the boundary condition (3.3).

Substituting Eq. (3.10) into Eq. (3.3) and using the formula corresponding to the Neumann's addition theorem [28]

$$xJ_1(x\rho)=\frac{8\rho}{(1-\lambda^2)\sin\alpha}\sum_{m=1}^{\infty} m J_m\left(x\frac{1+\lambda}{2}\right)J_m\left(x\frac{1-\lambda}{2}\right)\sin(m\alpha), \tag{3.12}$$

$$\lambda<\rho<1,$$

it is found that

$$\sum_{n=1}^{\infty} a_n\int_0^{\infty} Z_n(x)[1-M(x\eta)]\left[\sum_{m=1}^{\infty} mZ_m(x)\sin(m\alpha)\right]dx=\sin\alpha, \tag{3.13}$$

$$0<\alpha<\pi.$$

Since Eq. (3.13) must hold for an arbitrary value of α, we find that the equation is reduced to the following infinite system of simultaneous algebraic equations for the determination of the unknown coefficients a_n

$$\sum_{n=1}^{\infty} a_n A_{mn}=\delta_{1m}, \quad m=1,2,3,\ldots, \tag{3.14}$$

in which δ_{1m} denotes the Kronecker delta, the matrix A_{mn} is symmetric with respect to m and n and is defined as follows:

$$A_{mn}=\int_0^{\infty}[1-M(x\eta)]Z_m(x)Z_n(x)\,dx, \quad m,n=1,2,3,\ldots. \tag{3.15}$$

After solving the infinite system of Eqs. (3.14), the displacement and stress states in the body and the fracture parameters can be derived.

The components of the stress and displacement at $\zeta=0$ are presented by Eqs. (2.23) and (3.10) with the aid of the dimensionless variables which are cited above.

The displacement at $\zeta=0$ is given by Eq. (3.11) and the radial gradient of one in $\lambda<\rho<1$ is

$$(3.16)\quad \frac{dv_\theta(\rho)}{bd\rho}=\frac{\tau_0 b(1-\lambda^2)}{8\pi G_{arg}}\left[\frac{4}{1-\lambda^2}\sum_{n=1}^{\infty}\frac{a_n\cos(n\alpha)}{\sin\alpha}+\right.$$

$$\left.-\frac{1}{\rho^2}\sum_{n=1}^{\infty}\frac{a_n\sin(n\alpha)}{n}\right],\quad \lambda<\rho<1,$$

and tends to infinity as $\rho\to\lambda+0$ or $\rho\to1-0$.

The stress components at $\zeta=0$ are

$$(3.17)\quad \sigma_{r\theta}(\rho)=\frac{\tau_0 bs(1-\lambda^2)}{4\pi}\left[\frac{2}{1-\lambda^2}\sum_{n=1}^{\infty}\frac{a_n\cos(n\alpha)}{\sin\alpha}-\frac{1}{\rho^2}\sum_{n=1}^{\infty}\frac{a_n\sin(n\alpha)}{n}\right],$$

$$(3.18)\quad \sigma_{z\theta}(\rho)=-\tau_0 b\rho,$$

in the crack surface $\lambda<\rho<1$ and

$$(3.19)\quad \sigma_{r\theta}(\rho)=0,$$

$$(3.20)\quad \sigma_{z\theta}(\rho)=\frac{\tau_0 b(1-\lambda^2)}{8}\sum_{n=1}^{\infty}a_n\left[\frac{\partial I_0^n}{\partial\rho}+M_1^n\right],$$

outside the crack area $0\leqslant\rho<1$, $1<\rho$.

The integrals I_0^n and M_1^n are defined as follows:

$$(3.21)\quad I_0^n(\rho;\lambda)=\int_0^{\infty}J_0(x\rho)J_n\left(x\frac{1+\lambda}{2}\right)J_n\left(x\frac{1-\lambda}{2}\right)dx,\quad n=1,2,3,\ldots,$$

$$(3.22)\quad M_1^n(\rho;\lambda,\eta)=\int_0^{\infty}xM(x\eta)J_1(x\rho)J_n\left(x\frac{1+\lambda}{2}\right)J_n\left(x\frac{1-\lambda}{2}\right)dx,$$

$$n=1,2,3,\ldots.$$

The infinite integrals M_1^n are convergent because the functions $M(x\eta)$ have properties (2.21) and we can easily evaluate these integrals by a numerical method. The integrals (3.21) can be expressed by analytical expressions in terms of Gaussian hypergeometric series and a Gamma one [27, 11]. Their full expressions are given in the Appendix.

The stress $\sigma_{r\theta}(\rho)$ is nonzero only for $\lambda<\rho<1$, tending to infinity as $\rho\to\lambda+0$ and $\rho\to1-0$. The stress $\sigma_{z\theta}(\rho)$ is always positive for $0\leqslant\rho<\lambda$ or $\rho>1$ and tends to infinity as $\rho\to\lambda-0$ or $\rho\to1+0$. The singular part of $\sigma_{z\theta}(\rho)$ is included in the first term of Eq. (3.20) because $\partial I_0^n/\partial\rho$ has singular parts such as $(\lambda-\rho)^{-1/2}$ and $(\rho-1)^{-1/2}$, whereas the second term is continuous in all of ρ (see Appendix).

The displacement and stress distributions in the interior of the layer can be obtained by the numerical integrations of equations derived by making the substitutions of Eq. (3.10) into Eqs. (2.17).

In terms of the quantity a_n actually calculated, the fracture mechanics parameters, the crack energy and the stress intensity factors of the inner and outer tips of the crack, can be studied.

The strain energy of the crack is defined by

$$W=2\pi \int_a^b \tau_0 v_\theta (r, 0) r^2 \, dr, \tag{3.23}$$

or, using Eq. (3.11), is given as

$$W=\frac{\pi \tau_0^2 b^5 (1-\lambda^2)^2}{32 G_{\text{arg}}} a_1. \tag{3.24}$$

To determine the stress intensity factors (SIFs), we consider the stress behaviour near the crack edges and their singularity at the crack tips into material regions omitting the hypergeometric function (see Appendix).

The stresses $\sigma_{z\theta}(\rho)$ are rewritten as follows:

$$\sigma_{z\theta}(\rho)=\frac{\tau_0 b (1-\lambda^2)}{8} \sum_{n=1}^{\infty} a_n \left[M_1^n - \int_0^\infty x J_1 (x\rho) Z_n (x) \, dx\right]. \tag{3.25}$$

Using the asymptotic expansion of $J_n (x\rho)$ with a large value of x [28]

$$J_n (x\rho) \doteq \sqrt{\frac{2}{\pi x\rho}} \cos\left(x\rho - \frac{2n+1}{4}\pi\right), \tag{3.26}$$

we obtain

$$xZ_n (x) \doteq \frac{2}{\pi \sqrt{1-\lambda^2}} [\cos \lambda x + (-1)^n \sin x]. \tag{3.27}$$

Then we decompose the stress $\sigma_{z\theta}(\rho)$ into parts as follows:

$$\sigma_{z\theta}(\rho)=\frac{1}{8} \tau_0 b (1-\lambda^2) \sum_{n=1}^{\infty} a_n \left\{M_1^n - \int_0^\infty \left[xZ_n (x) - \frac{2}{\pi \sqrt{1-\lambda^2}} (\cos \lambda x + (-1)^n \sin x)\right] J_1 (x\rho) \, dx - \frac{2}{\pi \sqrt{1-\lambda^2}} \cdot \frac{1}{\rho} \left[1 - \frac{\lambda H(\lambda-\rho)}{\sqrt{\lambda^2-\rho^2}} + (-1)^n \frac{H(\rho-1)}{\sqrt{\rho^2-1}}\right]\right\}, \tag{3.28}$$

with the aid of the properties of the integrals [27–28]

$$\int_0^\infty \cos(\lambda x) J_1 (x\rho) \, dx = \frac{1}{\rho}\left[1 - \frac{\lambda H(\lambda-\rho)}{\sqrt{\lambda^2-\rho^2}}\right],$$
$$\int_0^\infty \sin x J_1 (x\rho) \, dx = \frac{H(\rho-1)}{\rho \sqrt{\rho^2-1}}, \tag{3.29}$$

where $H(x)$ is a step function.

The singular part of the stress $\sigma_{z\theta}(\rho)$ is included in the last term of Eq. (3.28). Consequently, the stress intensity factors corresponding to torsion at the inner and the outer edges of the crack are defined by the limits

$$K_a^T = \lim_{\rho\to\lambda-} \sqrt{2b(\lambda-\rho)}\ \{\sigma_{z\theta}(\rho)\}_{\rho<\lambda}, \qquad K_b^T = \lim_{\rho\to 1+} \sqrt{2b(\rho-1)}\ \{\sigma_{z\theta}(\rho)\}_{\rho>1}, \tag{3.30}$$

or in terms of the quantity actually calculated:

$$K_a^T = \frac{1}{4\pi}\tau_0 b^{3/2}\sqrt{\frac{1-\lambda^2}{\lambda}}\sum_{n=1}^{\infty} a_n,$$
$$K_b^T = \frac{1}{4\pi}\tau_0 b^{3/2}\sqrt{1-\lambda^2}\sum_{n=1}^{\infty}(-1)^{n+1} a_n. \tag{3.31}$$

On the other hand, it is easy to see from the behaviour of $Z_n\left(x, \frac{1+\lambda}{2}, \frac{1-\lambda}{2}\right)$ that if $\lambda\to 1-2\varepsilon$ (ε — a small value), then the SIFs become equal and tend to

$$K_a^T \to K_b^T = \tau_0 b^{3/2}\varepsilon^{1/2}, \qquad \lambda\to 1-2\varepsilon, \tag{3.32}$$

which is the solution for antiplane shear and tend to zero as ε is zero.

Using the result given later by Eq. (3.35) for a penny-shaped crack in an infinite homogeneous body, we have

$$\sum_{n=1}^{\infty} a_n = 0 \quad \text{and} \quad \sum_{n=1}^{\infty}(-1)^{n+1} a_n = \frac{16}{3}. \tag{3.33}$$

Consequently, in an infinite, homogeneous body, as $a/b\to 0$, K_b^T approaches the value

$$K_b^T = \frac{4}{3\pi}\tau_0 b^{3/2} \tag{3.34}$$

and $K_a^T = 0$.

It is seen that K_b^T is always greater than K_a^T, so it is to be expected that if growth of the crack occurs it will be at the outer edge.

The special case

In the special case of the infinite body ($M(x\eta)=0$, $\eta\to\infty$) and $\lambda\to 0$ (but b is bounded) from the above results, we obtain closed form solutions:

$$a_n = -\frac{512}{3\pi}\cdot\frac{n^2}{(4n^2-1)(4n^2-9)}, \tag{3.35}$$

$$xv(x) = -\frac{4}{\pi}\frac{\tau_0 b}{G_{arg}}\left[\frac{1}{x}\frac{d}{dx}\left(\frac{\sin x}{x}\right)+\frac{1}{3}\frac{\sin x}{x}\right],$$
$$v_\theta(\rho) = \frac{4}{3\pi}\frac{\tau_0 b^2}{G_{arg}}\rho\sqrt{1-\rho^2}\,H(1-\rho), \tag{3.36}$$

$$\sigma_{z\theta}(\rho)=\frac{4}{3\pi}\tau_0 b\left[\left(3\rho-\frac{2}{\rho}\right)\frac{1}{\sqrt{\rho^2-1}}+\frac{3}{2}\left(\rho\arccos\left(\frac{1}{\rho}\right)+\right.\right.$$

$$\left.\left.-\frac{\sqrt{\rho^2-1}}{\rho}\right)\right]H(\rho-1), \tag{3.37}$$

$$\sigma_{r\theta}(\rho)=\frac{4}{3\pi}\tau_0 bs\frac{\rho^2}{\sqrt{1-\rho^2}}H(1-\rho),$$

$$W=\frac{16}{45}\frac{\tau_0^2 b^5}{G_{\text{arg}}},\quad K_a^T=0,\quad K_b^T=\frac{4}{3\pi}\tau_0 b\sqrt{b}. \tag{3.38}$$

The results (3.37) and (3.38) agree with those in the case of the penny-shaped crack [4]. For the classical case (but of the material with two shear moduli), the displacement v_θ and the strain energy depend on the average shear modulus while the stress $\sigma_{r\theta}$ depends on the material parameter $s=\sqrt{G/G_z}$. In this case the stress $\sigma_{z\theta}$ and the stress intensity factor are independent of anisotropy of the material.

4. A TRANSVERSELY ISOTROPIC LAYER UNDER TORSION BY A ELAT ANNULAR RIGID PUNCH

We consider a transversely isotropic layer occupying the region $0\leqslant r<\infty$, $0\leqslant z\leqslant h$, $0\leqslant\theta\leqslant 2\pi$ and a rigid, flat, annular punch attached to the portion $z=0$ and $a\leqslant r\leqslant b$ for all θ, where a and b are the inner and outer radii of the annulus. We denote the torque applied to the annulus and the angle of rigid rotation by T and ω_0, respectively. The load is applied in the z-direction, the rest of the plane surface $z=0$ is stress free. The lower edge of the layer is elastically or rigid clamped or bonded to a half-space $z\geqslant h$. It should be noted that the boundary condition for the case $k\to\infty$ (rigid clamped edge) is equivalent to the torsional indentation of a layer by a pair of the same annulus centrally embedded onto both surfaces of one. Then the boundary conditions in dimensionless coordinates are as follows:

$$\sigma_{z\theta}(\rho,0)=0,\quad 0\leqslant\rho<\lambda,\quad 1<\rho, \tag{4.1}$$

$$v_\theta(\rho,0)=\omega_0 b\rho,\quad \lambda\leqslant\rho\leqslant 1,\quad \lambda=a/b. \tag{4.2}$$

The angle of rotation ω_0 is obtained from the equilibrium equation of the punch

$$T=-2\pi b^3\int_\lambda^1\sigma_{z\theta}(\rho,0)\rho^2\,d\rho. \tag{4.3}$$

Using Eqs. (2.24), we see that $t(x)$ is the only unknown which from Eqs. (4.1) and (4.2) can be found from the triple integral equations

$$\int_0^\infty xt(x)J_1(x\rho)\,dx=0,\quad 0\leqslant\rho<\lambda,\quad 1<\rho, \tag{4.4}$$

$$\int_0^\infty t(x)[1-H(x\eta)]J_1(x\rho)\,dx=\omega_0 b^2\rho,\quad \lambda\leqslant\rho\leqslant 1, \tag{4.5}$$

where the function $H(x\eta)$ is given by the formulas (2.20). Following the similar method as in the previous section for solving Eqs. (4.4) and (4.5), it can be shown that using the formulas (3.8) and the conditions (4.4), we get

$$t(x)=\omega_0 b^2 \frac{1+\lambda^2}{2} \sum_{n=0}^{\infty} b_n \frac{\partial Z_n(x)}{\partial x}, \tag{4.6}$$

where to determine the unknown coefficients b_n we have the conditions (4.5). Substituting Eq. (4.6) into the boundary condition (4.5), using the relation $\partial J_0(x\rho)/\partial x=-\rho J_1(x\rho)$, the formula (3.5) and the Neumann's formula [28]

$$J_0(x\rho)=Z_0(x)+2\sum_{m=1}^{\infty} Z_m(x)\cos(m\alpha), \quad 0\leqslant\alpha\leqslant\pi, \tag{4.7}$$

and equating the coefficients of $\cos(m\alpha)$ at both sides, we obtain the infinite system of simultaneous algebraic equations with respect to the unknown coefficients b_n

$$\sum_{n=0}^{\infty} b_n B_{mn}=\delta_{0m}-\frac{1}{2}\left(1-\frac{2\lambda^2}{1+\lambda^2}\right)\delta_{1m}, \quad m=0, 1, 2, \ldots. \tag{4.8}$$

where

$$B_{mn}=\int_0^{\infty}[1-H(x\eta)]\frac{\partial}{\partial x}[Z_m(x)]\frac{\partial}{\partial x}[Z_n(x)]\,dx, \quad m, n=0, 1, 2\ldots \tag{4.9}$$

and the function $Z_n(x)$ is defined by Eq. (3.6).

Assuming the coefficients b_n as

$$b_n=b_n'-\frac{1}{2}\left(1-\frac{2\lambda^2}{1+\lambda^2}\right)b_n'' \tag{4.10}$$

Eqs. (4.8) are divided into two infinite systems of linear algebraic equations:

$$\sum_{n=0}^{\infty} b_n' B_{mn}=\delta_{0m}, \quad \sum_{n=0}^{\infty} b_n'' B_{mn}=\delta_{1m}, \quad m=0, 1, 2, \ldots, \tag{4.11}$$

where δ_{0m}, δ_{1m} are the Kronecker delts and B_{mn} are given by the convergent infinite integrals (4.9). The present mixed boundary value problem is reduced to the solution of an infinite system of linear algebraic equations (4.8) or Eqs. (4.11).

The quantities of physical interest are obtained from Eqs. (2.24) on the surface of the layer and from Eqs. (2.18) in the interior of the solid by using the representation (4.6). In the half-space $z\geqslant h$ the displacement and stress components are calculated by Eqs. (2.6), (4.6) and (2.16) for $A(\xi)=C(\xi)$ and $i=0$.

The displacement at $\zeta=0$ is given by

$$v_0(\rho)=\begin{cases}\omega_0 b\rho, & \lambda\leqslant\rho\leqslant 1,\\ \dfrac{1}{2}\omega_0 b(1+\lambda^2)\displaystyle\sum_{n=0}^{\infty} b_n\left[\frac{1}{2}\rho(I_0^n-I_2^n)+h_1^n(\rho;\lambda,\eta)\right], & 0\leqslant\rho\leqslant\lambda, \quad 1\leqslant\rho.\end{cases} \tag{4.12}$$

The tangential contact stresses on the punch are

$$\sigma_{z\theta}(\rho)=-\frac{\omega_0(1+\lambda^2)G_{arg}}{\pi\sqrt{(\rho^2-\lambda^2)(1-\rho^2)}}\rho\sum_{n=0}^{\infty}b_n\cos n\alpha,\quad \lambda<\rho<1,\quad 0<\alpha<\pi, \tag{4.13}$$

where the angle α is given by the formula (3.5). The contact stresses on the punch are continuous at all points and tend to infinity as $\rho\to\lambda+0$ or $\rho\to1-0$. The second component of the tensor stress is zero inside the contact area and

$$\sigma_{r\theta}(\rho)=\frac{1}{2}G\omega_0(1+\lambda^2)\sum_{n=0}^{\infty}b_n\left[I_2^n+\rho\frac{\partial I_0^n}{\partial\rho}-H_2^n(\rho;\lambda,\eta)\right], \tag{4.14}$$

$$0\leqslant\rho<\lambda,\quad 1<\rho$$

outside the contact area. The stress $\sigma_{r\theta}(\rho)$ tends to infinity as $\rho\to\lambda-0$ or $\rho\to1+0$. This component of the stress is positive in $0\leqslant\rho<\lambda$ and negative in $\rho>1$ and tends to zero as $\rho\to\infty$, and is zero as $\rho=0$.

The integrals I_0^n and I_2^n are given by the formulas

$$I_l^n=\int_0^{\infty}J_l(x\rho)\,Z_n(x)\,dx,\quad l=0,2 \tag{4.15}$$

and are presented analytically in the Appendix.

The integrals $h_1^n(\rho;\lambda,\eta)$ and $H_2^n(\rho;\lambda,\eta)$ are defined as follows:

$$\{h_1^n, H_2^n\}=\int_0^{\infty}\{J_1(x\rho), xJ_2(x\rho)\}\,H(x\eta)\frac{\partial Z_n(x)}{\partial x}dx. \tag{4.16}$$

and these values are obtained by numerical integration. These integrals have very good convergence because the functions $H(x\eta)$ have the properties (2.21). From Eqs. (4.13) and (4.3) we have the value of the torque T required to maintain the angle of rotation ω_0

$$T=\frac{1}{2}\pi G_{arg}\omega_0 b^3(1+\lambda^2)^2\left[b_0-\frac{1}{2}\left(1-\frac{2\lambda^2}{1+\lambda^2}\right)b_1\right]. \tag{4.17}$$

The special case

In the special case of the half-space $(H(x\eta)=0,\ \eta\to\infty)$ and $\lambda\to0$ (but b is bounded), we have the closed-form solutions:

$$b_0=\frac{8}{\pi},\quad b_n=-\frac{16}{\pi}\cdot\frac{1}{4n^2-1},\quad n=1,2,3,\ldots, \tag{4.18}$$

$$t(x)=\frac{4}{\pi}\omega_0 b^2\left(\frac{\cos x}{x}-\frac{\sin x}{x^2}\right),$$

$$\omega_0=\frac{3T}{16b^3G_{arg}}, \tag{4.19}$$

$$v_\theta(\rho)=\frac{3T}{16b^2 G_{arg}}\rho\left\{1-\left[\frac{2}{\pi}\arcsin\left(\frac{1}{\rho}\right)+\frac{1}{\rho}\sqrt{\rho^2-1}\right]H(\rho-1)\right\},$$

$$\sigma_{z\theta}(\rho)=-\frac{3T}{4\pi b^3}\cdot\frac{\rho}{\sqrt{1-\rho^2}}H(1-\rho),\qquad \sigma_{r\theta}(\rho)= \tag{4.20}$$

$$=-\frac{3T}{4\pi b^3}\sqrt{\frac{G}{G_z}}\cdot\frac{\rho^{-2}}{\sqrt{\rho^2-1}}H(\rho-1),$$

where $H(\rho)$ is a Heavyside's step function.

The results (4.20) agree with the ones for the isotropic case of circular rigid punch, given by SNEDDON [2]. For the classical case, but of a material with two shear moduli, the angle of rotation and the displacement v_θ are dependent on the average shear modulus. In this case the contact stress is independent of the anisotropy of the material, whereas the stress $\sigma_{r\theta}(\rho)$ dependes on the material parameter $s=\sqrt{G/G_z}$.

5. NUMERICAL CALCULATIONS

After solving two infinite systems of algebraic equations (3.14) for the crack problem and Eqs. (4.8) or (4.11) for the contact problem, we obtain the quantities of physical interest in both problems. At first we must evaluate the infinite integrals in these equations. The elements A_{mn} and B_{mn} of m-th row and n-th column can be rewritten, with the aid of the asymptotic formulas (3.26) and (3.27), as

$$A_{mn}\approx\int_0^\beta Z_m(x)\,Z_n(x)\,dx-\int_0^\gamma M(x\eta)\,Z_m(x)\,Z_n(x)\,dx+\frac{4}{\pi^2(1-\lambda^2)}\times \tag{5.1}$$

$$\times\left\{\frac{\cos^2\lambda\beta}{\beta}+\lambda si(2\lambda\beta)+(-1)^{m+n}\left[\frac{\sin^2\beta}{\beta}-si(2\beta)\right]+[(-1)^m+(-1)^n]\times\right.$$

$$\left.\times\left[\frac{\sin\beta\cos\lambda\beta}{\beta}-\frac{1}{2}(1+\lambda)\,ci[\beta(1+\lambda)]-\frac{1}{2}(1-\lambda)\,ci[\beta(1-\lambda)]\right]\right\},$$

$$B_{mn}\approx\int_0^\beta\frac{\partial}{\partial x}[Z_m(x)]\frac{\partial}{\partial x}[Z_n(x)]\,dx-\int_0^\gamma H(x\eta)\frac{\partial}{\partial x}[Z_m(x)]\frac{\partial}{\partial x}\times \tag{5.2}$$

$$\times[Z_n(x)]\,dx+\frac{4}{\pi^2(1-\lambda^2)}\left\{\frac{\lambda^2\sin^2\lambda\beta}{\beta}-\lambda^3 si(2\lambda\beta)+(-1)^{m+n}\left[\frac{\cos^2\beta}{\beta}+\right.\right.$$

$$\left.+si(2\beta)\right]-\lambda[(-1)^m+(-1)^n]\left[\frac{\sin\lambda\beta\cos\beta}{\beta}-\frac{1}{2}(1+\lambda)\,ci[\beta(1+\lambda)]+\right.$$

$$\left.\left.+\frac{1}{2}(1-\lambda)\,ci[\beta(1-\lambda)]\right]\right\},$$

where β is a very large value, γ is a large value and $si(x)$, $ci(x)$ denote the integral sine and cosine functions, respectively. We can get numerically good results, taking $\beta=500$ and $\gamma=10/s\eta$. The integrals in Eqs. (5.1) and (5.2) are evaluated by means

of Simpson's numerical integral formula. The simultaneous algebraic equations are solved by truncation and we can get numerically good results taking only first n roots, where $n=15$ in the case of $\lambda \leqslant 0{,}2$ and $n=10$ in $\lambda > 0{,}2$ for $\eta > 1$ and $s > 1$, and $n=20$ or $n=15$ in the case $\lambda \leqslant 0{,}2$ or $\lambda > 0{,}2$ as $\eta \leqslant 1$ and $s \leqslant 1$, respectively.

6. Numerical results

For example, in an transversely-isotropic laminate composite (G', G_z') containing a layer (G, G_z) with a crack ($\lambda=0.5$) and equal to the average shear modulus, and arbitrary s and s', we obtain for the stress $\sigma_{z\theta}(\rho)$ in the neighbourhood of the crack tips the following results:

Table 1. The variation of $\sigma_{z\theta}(\rho)/\tau_0 b$ with n and ρ.

ρ	$n=10$	$n=15$	$n=20$
0.48	1.139399	1.139445	1.139442
0.49	1.797122	1.797170	1,797178
1.005	3.053311	3.053526	3.053384
1.03	0.843882	0.843956	0.843955

We confirm in Table 1 that the stress $\sigma_{z\theta}(\rho)$ is in good agreement for each case of $n=10$, 15 and 20.

Table 2. The values of the material parameters.

	$s^2=G/G_z$	G_{arg}/G_{isotr}
I. Cadmium	2.25	2.33
II. Magnesium	1.03	1.65
III. E galass-epoxy	0.98	0.46
IV. Graphite-epoxy	0.68	0.34
V. Isotropy	1.0	1.0

$G_{isotr}=10^{11}$ dynes/cm$^2=G_t$

Table 2 lists the material parameters of the four anisotropic materials and one isotropic material used in the computation, which are taken from references (29, 30].

In Figs. 1–5, dotted, solid, chain and double dotted chain lines are used to indicate the results for I, II, III, IV materials, respectively, and the results indicated by the mark x show those for the isotropic case. Figure 1 shows the variation of $v_\theta(\rho)$ with λ for $\eta \geqslant 2$ and stress-free edges. The value of v_θ gradually approaches the one for a penny-shaped crack when $\lambda \to 0$. Figure 2 shows the effect of anisotropy on v_θ. With an increasing s and G_{arg}/G_{isotr} v_θ decreases. In Fig. 3 we show the variation of $v_{\theta max}$ for $\kappa_t=0$ with a layer thickness ($\eta=h/b$). When $s\eta \geqslant 2$, $v_{\theta max}$ approaches to the one for the infinite solid.

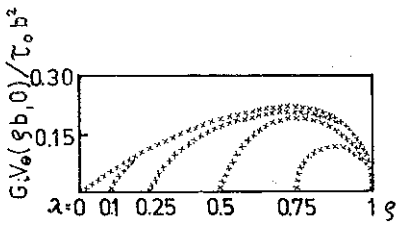

FIG. 1. The variation of v_θ with λ for $\eta \geqslant 2$ and $\kappa_1 = 0$.

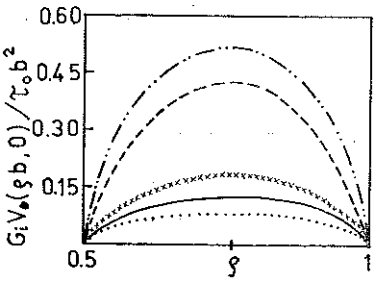

FIG. 2. The effect of anisotropy on v_θ for $\lambda = 0.5$, $\eta \geqslant 2$ and $\kappa_1 = 0$.

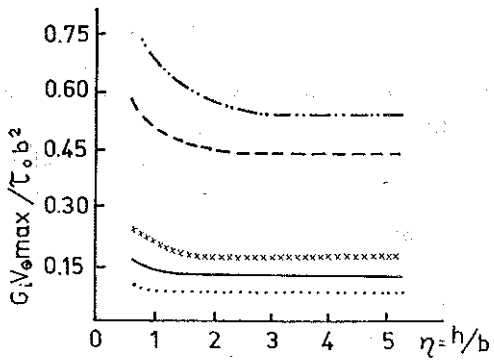

FIG. 3. The variations of $v_{\theta\max}$ with a layer thickness.

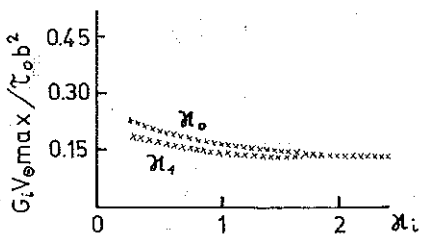

FIG. 4. The effect of boundary conditions on $v_{\theta\max}$ for $\eta = 1$.

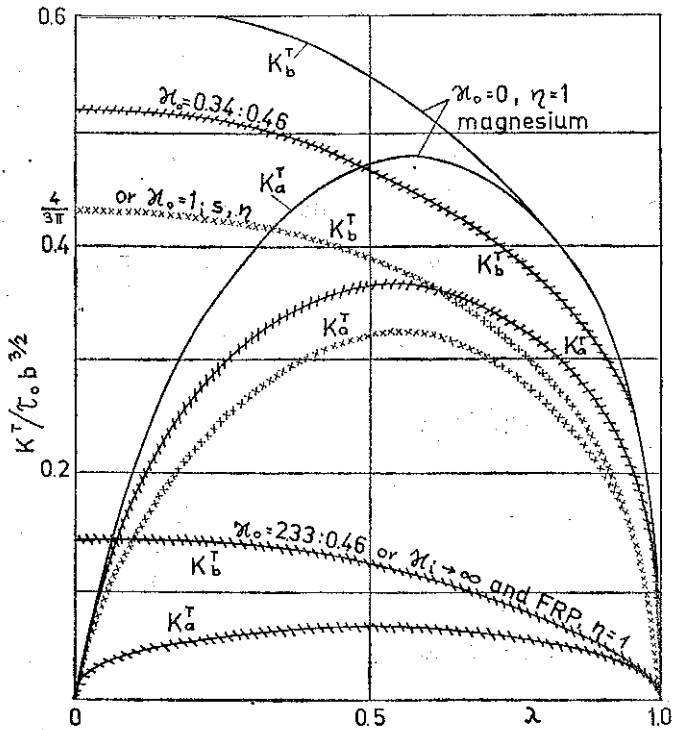

FIG. 5. The variation of K^T with λ for dissimilar materials and boundary conditions ($\eta=1$).

Figure 4 shows the effect of boundary conditions on $v_{\theta\max}$ for $\eta=1$. The displacement $v_{\theta\max}$ decreases with an increasing κ_i. When $\kappa_1>2$ and $\kappa_0>2$, we have these same values of $v_{\theta\max}$. The variations of the stress intensity factors are shown in Fig. 5. The value of K_b^T at the outer edge is always greater than K_a^T at the inner edge, so it is to be expected that if growth of the crack occurs, it will be at the outer edge. These values increase as κ_i decrease. The broken lines ⤙ or ⤚ denote the results

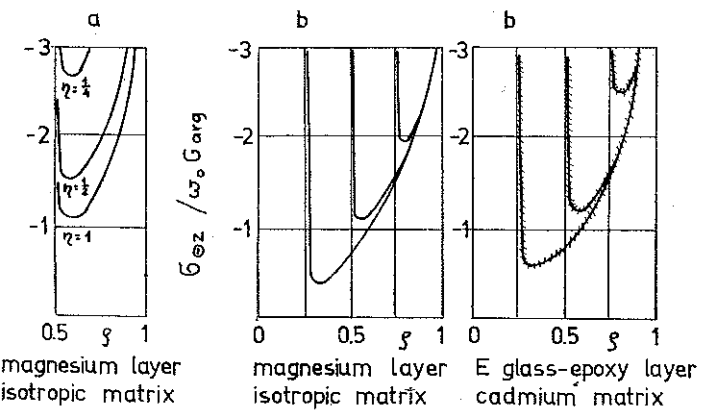

FIG. 6. The distribution of $\sigma_{z\theta}$ (ρb, 0) for various values of η ($\lambda=0.5$) (a) and of ρ ($\eta=1$) (b).

for layered composites: the cracked layer is with glass-epoxy and the surrounding material is cadmium or graphite-epoxy, respectively.

Figure 6a shows the distributions of contact stress $\sigma_{z\theta}(\rho)$ for various thicknesses of the plate under $\lambda=0.5$ and $\kappa_0=1$. The contact stress decreases as the thickness of the layer becomes large. Figure 6b shows the radial distributions of $\sigma_{z\theta}(\rho)$ for various values of λ under $h/b=1, 0$. The contact stress becomes large with an increasing λ. These values correspond to the bi-material composite with $G_{arg}=G'_{arg}$ or to the isotropic case ($G_{arg}=G_i$).

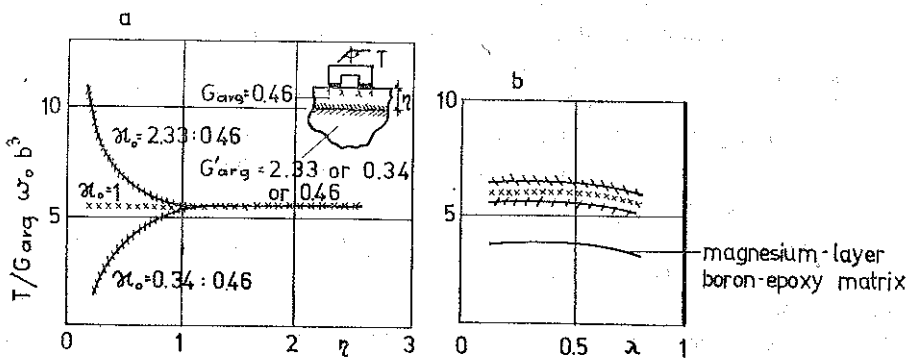

FIG. 7. The relation between the torque T and the ration η for $\lambda=0.5$ (a) or the ratio λ for $\eta=1.0$ (b).

Figure 7a shows the relations between the total torque T and the ratio $\eta=h/b$. Under the same magnitude of λ and $\kappa_0\gg1$, the torque T, taking a very large value in a thin layer, decreases as the thickness becomes large and tends to the results for the case $G'_{arg}=G_{arg}$. Figure 7b shows the relations between the torque T and the ratio λ. The torque T decreases with a decreasing of κ_0, increases with an increasing κ_0 and tends to the results for the case when $G'_{arg}=G_{arg}$.

7. CONCLUSIONS

The results obtained can be summarized as follows:

1. In general, the stress and displacement fields and the fracture mechanics parameters are a function of the crack or annulus dimensions, the layer thickness, the material properties of the composite and boundary conditions.

2. The maximum value of the tangential displacement of crack surface increases as the layer thickness decreases or the parameter κ_1 of the elastic clamped decreases. When the average shear modulus of the cracked layer is greater than that of the surrounding material (i.e. when $\kappa_0<1$), the displacement of the crack surface tends to increase as compared with the case $\kappa_0=1$ and increases as κ_0 decreases. The opposite is observed when the crack is in a softer material as compared with the outside material. When the material parameters G_{arg} and $s=(G/G_z)^{1/2}$ of the cracked layer, characterizing the effect of anisotropy, decrease under the same surrounding material or elastically clamped, the displacement of crack surface increases. When

$s\eta=sh/b\geqslant 2$, then the maximum of the displacement is approximately constant, i.e. it is independent of the boundary conditions, but depends on the material.

3. When the average shear modulus of the cracked layer is greater than that of the surrounding material ($\kappa_0<1$), the stress intensity factors tend to increase as compared with the case equal to the average shear modulus and increase as κ_0 decreases. The opposite is observed when the crack is in a softer material as compared with the outside material. When the average shear modulus of the cracked layer decreases and the parameter s of one increases, then the SIFs decrease for the layer on a weak foundation and when G_{arg} and s increase the SIFs increase for the layer on a strong foundation, tending to the results for a composite with such a layer that $G_{\text{arg}}=G'_{\text{arg}}$.

4. The contact stress increases with an increasing λ, κ_1 and κ_0 and decreases as the thickness of the layer becomes large, tending to the results of the half-space as $s\eta\geqslant 2$.

5. Under $\lambda=$const, the torque T, required to maintain the angle of rotation ω_0, takes a very large value in a thin plate and strong foundation and a small value in a thin plate and weak foundation. These values tend to the result for a bi-material composite with $G_{\text{arg}}=G'_{\text{arg}}$.

6. The convergence of the infinite integrals and the set of simultaneous equations in the numerical calculation become slower with a decreasing degree of anisotropy of the material.

Appendix

The integrals that appear in Eqs. (3.21) and (4.15) are defined as

a) $0\leqslant\rho<\lambda$

$$I_0^n=\frac{2}{\sqrt{\pi}}\cdot\frac{\Gamma[n+(1/2)]}{\Gamma(n+1)}\cdot\frac{1}{1+\lambda}\left(\frac{1-\lambda}{1+\lambda}\right)^n F\left(\frac{1}{2},\, n+\frac{1}{2};\, n+1;\, f_3(\lambda,\rho)\right)\times$$
$$\times F\left(\frac{1}{2},\, n+\frac{1}{2};\, 1;\, f_4(\lambda,\rho)\right),$$

$$\frac{\partial I_0^n}{\partial\rho}=\frac{2\rho}{\sqrt{\pi}}\cdot\frac{\Gamma[n+(3/2)]}{\Gamma(n+1)}\,\frac{1}{(1+\lambda)^3}\left(\frac{1-\lambda}{1+\lambda}\right)^n\left(\frac{1+\rho}{\lambda+\rho}+\frac{\lambda-\rho}{1-\rho}\right)\times$$
$$\times\left[\frac{(1-\rho)(\lambda+\rho)}{(1+\rho)(\lambda-\rho)}\right]^{1/2}\left[\frac{f_1(\lambda,\rho)}{n+1}F\left(\frac{3}{2},\, n+\frac{3}{2};\, n+2;\, f_3(\lambda,\rho)\right)F\left(\frac{1}{2},\, n+\right.\right.$$
$$\left.+\frac{1}{2};\, 1;\, f_4(\lambda,\rho)\right)+f_2(\lambda,\rho)\,F\left(\frac{1}{2},\, n+\frac{1}{2};\, n+1;\, f_3(\lambda,\rho)\right)F\left(\frac{3}{2},\, n+$$
$$\left.+\frac{3}{2};\, 2;\, f_4(\lambda,\rho)\right)\right],$$

$$I_2^n=-\frac{2}{\sqrt{\pi}}\,\frac{\Gamma[n+(3/2)]}{\Gamma(n+1)}\cdot\frac{1}{(1+\lambda)^3}\left(\frac{1-\lambda}{1+\lambda}\right)^n\rho^2\,F\left(\frac{3}{2},\, n+\right.$$
$$\left.+\frac{3}{2};\, n+1;\, f_3(\lambda,\rho)\right)F\left(\frac{3}{2},\, n+\frac{3}{2};\, 3;\, f_4(\lambda,\rho)\right),$$

where

$$f_{1,2}(\lambda,\rho)=1\mp 2\rho\left(\frac{1+\rho}{\lambda+\rho}+\frac{\lambda-\rho}{1-\rho}\right)^{-1}\left[\frac{(1+\rho)(\lambda-\rho)}{(1-\rho)(\lambda+\rho)}\right]^{1/2},$$

$$f_{3,4}(\lambda,\rho)=\frac{1}{2}\left\{1-\frac{1}{(1+\lambda)^2}\left[4\sqrt{(\lambda^2-\rho^2)(1-\rho^2)}\mp((1-\lambda)^2-4\rho^2)\right]\right\}.$$

b) $\rho>1$

$$I_0^n=\frac{(-1)^n}{\pi}\left[\frac{\Gamma[n+(1/2)]}{\Gamma(n+1)}\right]^2\frac{1}{\rho^{2n+1}}\left(\frac{1-\lambda^2}{4}\right)^n F\left(n+\frac{1}{2},\ n+\right.$$

$$\left.+\frac{1}{2};\ n+1;\ f_7(\lambda,\rho)\right)F\left(n+\frac{1}{2},\ n+\frac{1}{2};\ n+1;\ f_8(\lambda,\rho)\right),$$

$$\frac{\partial I_0^n}{\partial\rho}=\frac{(-1)^{n+1}}{2\pi}\left[\frac{\Gamma[n+(3/2)]}{\Gamma(n+1)}\right]^2\frac{(1-\lambda^2)^n}{(n+1)\,4^n}\rho^{-2(n+2)}\left(\frac{\rho^2-\lambda^2}{\rho^2-1}\right)^{1/2}\times$$

$$\times\left[\frac{4(n+1)}{n+1/2}\rho^2\sqrt{\frac{\rho^2-1}{\rho^2-\lambda^2}}\,F\left(n+\frac{1}{2},\ n+\frac{1}{2};\ n+1;\ f_7(\lambda,\rho)\right)F\left(n+\frac{1}{2},\ n+\right.\right.$$

$$\left.+\frac{1}{2};\ n+1;\ f_8(\lambda,\rho)\right)+f_5(\lambda,\rho)\,F\left(n+\frac{3}{2},\ n+\frac{3}{2};\ n+2;\ f_7(\lambda,\rho)\right)F\left(n+\right.$$

$$\left.+\frac{1}{2},\ n+\frac{1}{2};\ n+1;\ f_8(\lambda,\rho)\right)+f_6(\lambda,\rho)\,F\left(n+\frac{1}{2},\ n+$$

$$\left.\left.+\frac{1}{2};\ n+1;\ f_7(\lambda,\rho)\right)F\left(n+\frac{3}{2},\ n+\frac{3}{2};\ n+2;\ f_8(\lambda,\rho)\right)\right],$$

$$I_2^n=\frac{(-1)^{n+1}}{\pi}\,\frac{n+1/2}{n-1/2}\left[\frac{\Gamma[n+(1/2)]}{\Gamma(n+1)}\right]^2\left(\frac{1-\lambda^2}{4}\right)^n\rho^{-(2n+1)}\times$$

$$\times F\left(n-\frac{1}{2},\ n+\frac{3}{2};\ n+1;\ f_7(\lambda,\rho)\right)F\left(n-\frac{1}{2},\ n+\frac{3}{2};\ n+1;\ f_8(\lambda,\rho)\right),$$

where

$$f_{5,6}(\lambda,\rho)=\left(1\mp\lambda\sqrt{\frac{\rho^2-1}{\rho^2-\lambda^2}}\right)^2,\qquad f_{7,8}(\lambda,\rho)=$$

$$=\frac{1}{2}-\frac{1}{2\rho^2}\left(\sqrt{(\rho^2-1)(\rho^2-\lambda^2)}\pm\lambda\right).$$

In the above expressions, the symbols $F(p,q;r;s)$ and $\Gamma(z)$ denote the Gaussian hypergeometric series and Gamma function, defined as follows;

$$F(p,q;r;s)=1+\sum_{n=1}^{\infty}\frac{\Gamma(p+n)\,\Gamma(q+n)\,\Gamma(r)}{\Gamma(p)\,\Gamma(q)\,\Gamma(r+n)}\,\frac{s^n}{n!}=$$

$$=1+\sum_{n=1}^{\infty}\frac{(p)_n\,(q)_n}{(r)_n}\cdot\frac{s^n}{n!};\qquad (p)_n=p\,(p+1)\,(p+2)\ldots(p+n-1),$$

$$\Gamma(z)=\int_0^{\infty}e^{-t}\,t^{z-1}\,dt,\qquad (z>0).$$

REFERENCES

1. E. REISSNER, H. SAGOCI, *Forced torsional oscillations of an elastic half-space*, J. Appl. Phys., **15**, 9, 652–654, 1944.
2. I. N. SNEDDON, *A note on a boundary value problem of Reissner and Sagoci*, J. Appl. Phys., **18**, 1, 130–132, 1947.
3. I. N. SNEDDON, *The Reissner-Sagoci problem*, Proc. Glasgow Math. Assoc., **7**, 136–144, 1966.
4. I. N. SNEDDON, M. LOWENGRUB, *Crack problems in the classical theory of elasticity*, John Wiley New York 1969.
5. В. С. Губенко, В. И. Моссаковский, *Давление осесимметричного кольцевого штампа на упругое полупространство*, ТММ, **20**, 2, 334-340, 1960.
6. Z. OLESIAK, *Annular punch on elastic semi-space*, Arch. Mech. Stos., **4**, 17, 633–648, 1965.
7. W. D. COLLINS, *The forced torsional oscillations of an elastic half-space and an elastic stratum*, Proc. London Math. Soc., **12**, 226–244, 1962.
8. J. C. COOKE, *Triple integral equations*, Quart. J. Mech. Appl. Math., **16**, 2, 193–203, 1963.
9. D. L. JAIN, R. P. KANWAL, *Torsional oscillations of an elastic half-space due to an annular disk and related problems*, Int. J. Engng Sci., **8**, 687–698, 1970.
10. T. SHIBUYA, *A mixed boundary value problem of an elastic half-space under torsion by a flat annular rigid stamp*, Bull. JSME, **19**, 129, 233–238, 1976.
11. T. SHIBUYA, I. MAKAHARA, T. KOIZUMI, *The axisymmetric distribution of stresses in an infinite elastic solid containing a flat annular crack under internal pressure*, ZAMM, **55**, 395–402, 1975.
12. T. SHIBUYA, I. NAKAHARA, T. KOIZUMI, *The axisymmetric stress distribution in an infinite elastic solid containing a flat annular crack under torsion*, Bull. JSME, **19**, 134, 853–862, 1976.
13. L. W. MOSS, A. S. KOBAYASHI, *Approximate analysis of axisymmetric problems in fracture mechanics with application to a flat toroidal crack*, Int. J. Fract. Mech., **7**, 89–99, 1971.
14. Б. И. Счетанин, *Задача о растяжении упругого пространства, содержащего плоскую кольцевую щель*, ПММ, **32**, 3, 458-462, 1968.
15. B. ROGOWSKI, *Pierścieniowa szczelina w ciele poprzecznie izotropowym*, ZN PŁ, 370, Budownictwo, z. 27 45–61, 1981.
16. B. ROGOWSKI, *Annular punch on a transversely isotropic layer bound to a half-space*, Arch. Mech., **34**, 2, 119–126, 1982.
17. M. DAHAN, *Stress distribution in a transversely isotropic solid containing a penny-shaped crack*, Arch. Mech., **33**, 3, 415–428, 1981.
18. Ya. KIZYMA, V. B. RUDNITSKII, *Stress-strain state of an elastic cylinder and a layer in joint torsion*, Arch. Mech., **25**, 3, 411–420, 1973.
19. V. B. RUDNITSKII, D. V. GRILITSKII, *Torsion of a double-layer isotropic medium by an annular punch*, Arch. Mech., **23**, 5, 651–661, 1971.
20. W. E. WILLIAMS, *Integral equation formulation of some three part boundary value problems*, Proc. Edinb. Math. Soc. (2), **13**, 317–323, 1963.
21. Z. OLESIAK, J. KOKOT, *A note on stress singularities in torsion by a rigid annulus*, Int. J. Engng. Sci., **18**, 1, 205–209, 1980.
22. A. Z. H. HASSAN, *Reissner-Sagoci problem for a nonhomogeneous large thick plate*, J. Mecanique, **18**, 1, 197–206, 1979.
23. Г. М. Валов, *Бесконечный упругий слой и полупространство под действием кольцевого штампа*, ПММ, **32**, 5, 894-907, 1968.
24. T. SHIBUYA, T. KOIZUMI, I. NAKAHARA, S. TANAKA, *The stress distribution in a thick elastic plate under torsional displacements by a pair of annular rigid punches*, Bull. JSME ,**20**, 144, 675–679, 1977.
25. R. S. DHALIWAL, B. M. SINGH, *Torsion by a circular die of a nonhomogeneous elastic layer bound to a nonhomogeneous half-space*, Int. J. Engng Sci., **16**, 9, 649–658, 1978.
26. B. ROGOWSKI, *Funkcje przemieszczeń dla ośrodka poprzecznie izotropowego*, Mech. Teor. i Stos., **13**, 1, 69–83, 1975.

27. A. ERDELYI (Editor), *Tables of integral transform*, Vol. 2, Mc Graw-Hill, New York 1954.
28. G. N. WATSON, *A treatise on the theory of Bessel function*, Cambridge 1944.
29. H. B. HUNTINGTON, *The elastic constants of crystals*, *Solid state physics* (F. Seitz, D. Turnbull, Eds.), 7, 213–351, Academic Press, New York 1957.
30. C. H. CHEN, S. CHENG, *Mechanical properties of anisotropic fiber-reinforced composites*, J. Appl. Mech., 37, 1, 186–189, 1970.

STRESZCZENIE

MIESZANE ZAGADNIENIA BRZEGOWE POPRZECZNIE IZOTROPOWEJ WARSTWY SKRĘCANEJ PRZY RÓŻNYCH WARUNKACH BRZEGOWYCH

Praca związana jest z zagadnieniem osiowo symetrycznego skręcania poprzecznie izotopowej warstwy podpartej sprężyście na dolnej płaszczyźnie lub połączonej z różną od niej półprzestrzenią. Rozpatrzono dwa typy potrójnych mieszanych zagadnień brzegowych: zagadnienie płaskiej, pierścieniowej szczeliny skręcanej i skręcanie warstwy za pomocą sztywnego pierścienia. Przedstawiono graficznie wyniki numerycznych obliczeń i sformułowano wnioski.

Резюме

СМЕШАННЫЕ КРАЕВЫЕ ЗАДАЧИ ТРАНСВЕРСАЛЬНО-ИЗОТРОПНОГО СЛОЯ СКРУЧИВАЕМОГО ПРИ РАЗНЫХ ГРАНИЧНЫХ УСЛОВИЯХ

Работа связана с задачей осесимметричного скручивания трансверсального-изотропного слоя упруго подпертого на нижней плоскости или соединенного с отличающегося от него полупространством. Рассмотрены два типа тройных смешанных краевых задач: задача плоской, скручиваемой кольцевой трещины и скручивание слоя при помощи жесткого кольца. Графически представлены результаты численных расчетов и сформулированы выводы.

TECHNICAL UNIVERSITY OF ŁÓDŹ
INSTITUTE OF CONSTRUCTION ENGINEERING

Received May 25, 1982.